

ORIGINAL ARTICLE

Induction of immunogenic cell death in murine colon cancer cells by ferrocene-containing redox phospholipid polymers

Masahiro Kaneko  | Akio Yamaguchi | Akira Ito 

Department of Chemical Systems
Engineering, School of Engineering,
Nagoya University, Nagoya, Japan

Correspondence

Masahiro Kaneko and Akira Ito,
Department of Chemical Systems
Engineering, School of Engineering,
Nagoya University, Furo-cho, Chikusa-ku,
Nagoya 464-8603, Japan.
Emails: kaneko.masahiro@material.nagoya-u.ac.jp (MK); ito.akira@material.nagoya-u.ac.jp (AI)

Funding information

Japan Society for the Promotion
of Science, Grant/Award Number:
20K22465; The Nitto Foundation; The
Public Interest of Tatematsu

Abstract

Immunogenic cell death (ICD), activated by damage-associated molecular patterns (DAMPs), is an apoptotic cell death process that elicits antitumor immunity. Although anticancer drugs that can induce ICD are promising for cancer treatment, the design strategy for ICD inducers remains unclear. In this study, we demonstrated the cell-penetrating redox phospholipid polymer poly(2-methacryloyloxyethyl phosphorylcholine-co-vinyl ferrocene) (pMFC) inducing ICD in murine colon cancer CT26 cells. pMFC produced oxidative stress by extracting electrons from CT26 cells and induced the release of DAMPs, such as calreticulin, adenosine triphosphate, and high-mobility group box 1. Moreover, the injection of pMFC-treated CT26 cells inhibited tumor formation in subsequently challenged CT26 cells, indicating that pMFC elicited antitumor immunity through ICD. Using in vivo therapy, intratumoral injections of pMFC induced complete tumor regression in 20% (1/5) of mice. These results suggested that the redox phospholipid polymer provides a new option for ICD-inducing anticancer polymers.

KEYWORDS

cancer cells, immunogenic cell death, oxidative stress, phospholipid polymers, redox reactions

1 | INTRODUCTION

In recent years, ICD has attracted attention as a promising cancer treatment strategy. ICD in cancer cells is characterized by the release of molecules called DAMPs, which elicit cancer immunogenicity.¹⁻³ ICD-associated DAMPs include the exposure of CRT at the cell surface and the release of ATP and HMGB1. CRT is a chaperone protein originally present in the ER and acts as an “eat me” signal during ICD and facilitates engulfment by dendritic cells, leading to the presentation of cancer antigens.^{4,5} ATP acts as a “find me” signal and attracts dendritic cells and macrophages to dying cancer cells.^{6,7}

HMGB1 is a nonhistone chromatin protein that facilitates antigen processing and presentation by dendritic cells.^{8,9} Therefore, DAMPs promote the maturation of dendritic cells and the activation of T cells to establish antitumor immunity. Anticancer drugs that induce ICDs may effectively suppress the recurrence of metastatic cancers.

Previous studies have revealed that oxidative stress in the ER, referred to as the elevation of ROS level, can trigger ICD.^{1,10,11} Therefore, drugs that induce oxidative stress may be candidates for inducing ICD. For example, PDT is a promising approach for inducing ICD. In PDT, photosensitizers convert oxygen to ROS and effectively kill cancer cells, thereby inducing ICD.¹² Some conventional

Abbreviations: AIBN, α,α -azobis(isobutyronitrile); CRT, calreticulin; DAMPs, damage-associated molecular patterns; DMF, *N,N*-dimethylformamide; DPBS, Dulbecco's phosphate-buffered saline; ER, endoplasmic reticulum; GSH, glutathione; HMGB1, high-mobility group box 1; ICD, immunogenic cell death; MPC, 2-methacryloyloxyethyl phosphorylcholine; ox-pMFC, oxidized forms of pMFC; PDT, photodynamic therapy; PI, propidium iodide; pMFC, poly(MPC-co-VFC); red-pMFC, reduced forms of pMFC; rho, thiocarbonyl rhodamine B; rho-pMFC, rhodamine B-labeled pMFC; ROS, reactive oxygen species; SHE, standard hydrogen electrode; THF, tetrahydrofuran; VFC, vinyl ferrocene.

This is an open access article under the terms of the [Creative Commons Attribution-NonCommercial-NoDerivs](https://creativecommons.org/licenses/by-nc-nd/4.0/) License, which permits use and distribution in any medium, provided the original work is properly cited, the use is non-commercial and no modifications or adaptations are made.

© 2022 The Authors. *Cancer Science* published by John Wiley & Sons Australia, Ltd on behalf of Japanese Cancer Association.

anticancer drugs such as oxaliplatin¹² and doxorubicin¹³ have reportedly induced ICD. However, a viable strategy for the molecular design of anticancer drugs that can induce ICD remains elusive.¹⁴ Therefore, it is highly desirable to explore novel ICD inducers.

This study focused on water-soluble redox phospholipid polymers as candidates for ICD inducers. Redox phospholipid polymers are composed of MPC units and redox-active units. MPC units serve as cytocompatible and hydrophilic units that prevent protein adsorption and solubilize hydrophobic monomers.^{15,16} Although hydrophobic compounds can exhibit cytotoxic to living cells,¹⁷ we expect that copolymerization of MPC and redox-active monomers will enable the evaluation of anticancer activity derived genuinely from redox properties. Amphiphilic MPC polymers can penetrate mammalian cell membranes via a simple diffusion mechanism.^{18–20} Cell membrane permeability and redox activity enable redox phospholipid polymers to interfere with the intracellular redox state. The redox phospholipid polymer pMFC can oxidize intracellular redox species because the redox potential of pMFC ($E = +0.5$ V versus SHE)²¹ is higher than that of the intracellular redox species. Although ferrocene exhibits poor water solubility ($<50\mu\text{M}$),²² pMFC is soluble in water even at a concentration exceeding 100 mg/ml, which corresponds to approximately 0.2 M ferrocene.²¹ Recently, it was reported that pMFC can induce oxidative stress by depleting the intracellular reducing power in human breast cancer cells.^{23,24} In the present study, we investigated whether pMFC could induce ICD in CT26 cells (Figure 1) and examined the therapeutic effects of pMFC.

2 | MATERIALS AND METHODS

2.1 | Materials

MPC, VFc, methacryloxyethyl rho, and AIBN were purchased from NOF, FUJIFILM Wako Pure Chemical, Polyscience, and Kanto Chemical, respectively. All organic reagents and solvents used in this study were commercially available reagents of extrapure grade and used without further purification.

2.2 | Synthesis of pMFC

pMFC and rho-pMFC were synthesized using conventional free radical polymerization, as previously reported^{21,23} with a slight modification. For the synthesis of pMFC, MPC (3.54 g), VFc (1.70 g), and

AIBN (164 mg) were dissolved in 20 ml ethanol:THF (80:20, v/v). After argon purging, polymerization was performed in a test tube at 65°C for 48 h. The test tube was cooled to $\sim 25^\circ\text{C}$ to stop polymerization. The polymer solution was precipitated using a mixed solvent composed of diethyl ether:chloroform (90:10, v/v).

For the synthesis of rho-pMFC, MPC (3.54 g), VFc (1.70 g), rho (130 mg), and AIBN (164 mg) were dissolved in 20 ml ethanol:THF (80:20, v/v). After argon purging, polymerization was performed in a test tube at 65°C for 48 h. The test tube was cooled to $\sim 25^\circ\text{C}$ to stop polymerization. The polymer solution was then precipitated using diethyl ether. The polymer precipitate was filtered and dissolved in a mixed solvent composed of methanol:water (1:1, v/v) and 1.0 M NaCl. The polymer solution was added to diethyl ether again, and the diethyl ether was subsequently removed by decantation. The remaining polymer solution was re-precipitated using DMF. The precipitate was washed with DMF repeatedly until the supernatant became colorless.

Both the precipitated polymers were collected and dissolved in distilled water. The polymer solutions were dialyzed with a Spectra/Por 7 Membrane (MWCO 1000 Spectrum Laboratories Inc.) for 4 days. The polymers were then freeze dried and the resulting powders were obtained as pMFC and rho-pMFC. Molecular weights were measured by gel permeation chromatography using poly(ethylene glycol) as a standard. The composition was determined using UV-vis spectroscopy (Table S1).

2.3 | Cell culture

CT26 cells were purchased from the American Type Culture Collection (ATCC). CT26 cells were seeded into 100-mm dishes with 1.0×10^6 cells/dish in 10 ml of RPMI 1640 (FUJIFILM Wako Pure Chemical) supplemented with 1% penicillin–streptomycin (FUJIFILM Wako Pure Chemical) and 10% FBS (Funakoshi), and cultured at 37°C in 5% CO₂.

2.4 | Internalization of pMFC into CT26 cells

CT26 cells were seeded in 2.0 ml RPMI 1640 at 2.0×10^5 cells/dish in glass-bottomed dishes (Iwaki Glass) and incubated for 1 day. A stock solution of rho-pMFC in DPBS (Thermo Fisher Scientific) was added to the cell cultures to obtain a final concentration of 1.0 mg/ml. The cells were incubated for 1 h at 37°C in 5% CO₂, and the cell culture

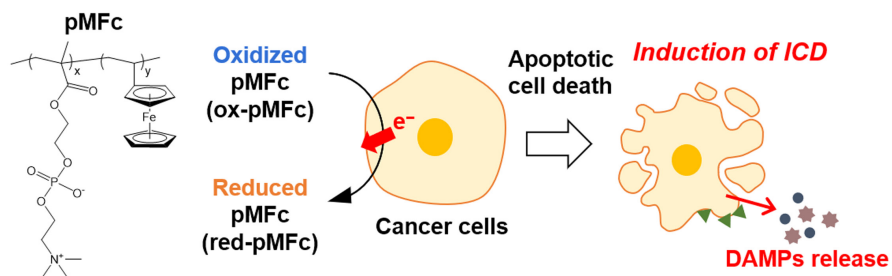


FIGURE 1 Schematic illustration of the induction of immunogenic cell death by redox phospholipid polymer pMFC

was washed twice with 2 ml of HBSS (Thermo Fisher Scientific) and replaced with 2 ml of fresh RPMI 1640 medium. Cells were imaged using an All-in-One Fluorescence Microscope BZ-X810 (Keyence). The fluorescence of the rho units in the polymer was measured using a tetramethylrhodamine (TRITC) filter (Keyence).

2.5 | Electrochemical oxidation of pMFC

pMFC was dissolved in DPBS at a concentration of 10 mg/ml. The pMFC solution was oxidized (at +0.60V versus SHE) with a potentiostat (VMP3, BioLogic) for several hours with stirring until the anodic current reached a plateau to obtain an ox-pMFC solution.

2.6 | Changes in the redox state of pMFC in CT26 cell culture

CT26 cells were seeded into 10 ml of RPMI 1640 medium in a 100-mm dish at 1.0×10^6 cells/dish and cultured for 24 h. The ox-pMFC solution in DPBS was added to obtain a final concentration of 1.0 mg/ml. The absorbance of the supernatant at 625 nm was measured using UV-vis spectroscopy and the ratio of ox-pMFC was calculated.

2.7 | Evaluation of oxidative stress

Oxidative stress was assessed using a CellROX Green Flow Cytometry Assay Kit (Thermo Fisher Scientific). CT26 cells were seeded in 6-well plates at 7.5×10^4 cells/well in 2 ml of RPMI 1640 medium and preincubated for 24 h. A stock solution of either red-pMFC or ox-pMFC in DPBS was added to the cell culture to obtain a final concentration of 1.0 mg/ml. After 1 h of incubation, CT26 cells were collected using trypsin and suspended in RPMI 1640 medium at 1.0×10^5 cells/ml for each sample. Next, 2 μ l of CellROX solution was added to 1 ml of cell suspension and this was incubated at 37°C in the dark for 30 min. The fluorescence of each cell type was analyzed using flow cytometry (Accuri C6 Plus, BD).

2.8 | Evaluation of the viability of CT26 cells treated with pMFC

Cell viability was assessed using the Cell Counting Kit-8 (Dojindo). CT26 cells were seeded in 96-well plates at 2.5×10^3 cells/well in 100 μ l of RPMI 1640 medium and incubated for 24 h. Thereafter, 10 μ l of the stock solution of pMFC at various concentrations was added to each well. After 24 h of incubation, the cells were washed twice with 100 μ l HBSS and replaced with 100 μ l fresh RPMI 1640 medium. Finally, 10 μ l of Cell Counting Kit-8 solution was added to each well and the cells were incubated for 2 h. Absorbance at 450 nm was measured using a microplate reader (iMark Microplate Absorbance Reader, Bio-Rad Laboratories). Cell-free medium was used as a blank.

2.9 | Apoptosis assay

The apoptosis assay was performed using the FITC Annexin V Apoptosis Detection Kit with PI (BioLegend). CT26 cells were seeded in six-well plates at 7.5×10^4 cells/well in 2 ml of RPMI 1640 medium and incubated for 24 h. A stock solution of either red-pMFC or ox-pMFC in DPBS was added to the cell culture to obtain a final concentration of 1.0 mg/ml. After 24 h of incubation, supernatants were collected. Cells were collected using trypsin. The collected supernatants and cell suspensions were mixed and centrifuged at 500 g for 5 min. The cells were washed twice with HBSS and suspended in Annexin V Binding Buffer to obtain a cell concentration of 1.0×10^6 cells/ml. The cell suspensions (100 μ l) were mixed with 5 μ l of annexin V and 10 μ l of PI. The samples were vortexed and stained at 25°C in the dark for 15 min. Annexin V Binding Buffer (400 μ l) was then added and flow cytometry analysis was conducted using a flow cytometer (Accuri C6 Plus).

2.10 | Analysis of CRT on the cell surface of CT26 cells

CT26 cells were seeded in 60-mm dishes at 3.0×10^5 cells/dish in 4 ml of RPMI 1640 medium and incubated for 24 h. A stock solution of either red-pMFC or ox-pMFC in DPBS was added to the cell culture to obtain a final concentration of 1.0 mg/ml. After 24 h of incubation, the supernatants were collected. Cells were collected using trypsin. The collected supernatants and cell suspensions were mixed, and the number of cells was adjusted to 2.5×10^5 to 5.0×10^5 cells for each sample. The cell suspensions were centrifuged at 500 g for 5 min. The cells were washed twice with 2 ml of 5% BSA-PBS and suspended in 100 μ l of Cell Staining Buffer (BioLegend). The suspensions were mixed with 1 μ l of the primary antibody (1G6A7) (Novus Biologicals) and incubated at room temperature in the dark for 30 min. The cell suspensions were centrifuged at 500 g for 5 min. After washing them twice with 2 ml of Cell Staining Buffer, 100 μ l of Cell Staining Buffer were added. The cell suspensions were mixed with 2.5 μ l of phycoerythrin (PE) anti-mouse IgG2a secondary antibody (BioLegend) and incubated at room temperature in the dark for 30 min. The cell suspensions were centrifuged at 500 g for 5 min, washed twice with 2 ml of Cell Staining Buffer, and suspended in 300 μ l of Cell Staining Buffer. Each sample was analyzed using a flow cytometer (Accuri C6 Plus).

2.11 | Measurement of ATP concentration in the supernatant of CT26 cell culture

CT26 cells were seeded in six-well plates at 1.0×10^6 cells/dish in 1 ml RPMI 1640 medium and incubated for 24 h. The stock solution of either red-pMFC or ox-pMFC in DPBS was administered to the cell culture at a final concentration of 1.0 mg/ml. After a 24 h incubation, the supernatants were collected and centrifuged at 9,200 g for 5 min at 4°C. Thereafter, 100 μ l of the supernatant was mixed with

100 μ l CellTiter Glo (Promega) and incubated at room temperature for 10 min. The luminescence of each sample was measured using a luminometer (Lumat LB 9507; Berthold Technologies) and the ATP concentration in the supernatant of CT26 cell culture was determined.

2.12 | Measurement of HMGB1 concentration in the supernatant of CT26 cell culture

Measurement of HMGB1 concentration was performed using the HMGB1 ELISA Kit Exp (Sino-Test, Japan). CT26 cells were seeded into six-well plates at 1.0×10^6 cells/dish in 1 ml RPMI 1640 medium and incubated for 24 h. A stock solution of either red-pMFC or ox-pMFC in DPBS was added to the cell culture to obtain a final concentration of 1.0 mg/ml. After a 24 h incubation, the supernatants were collected and centrifuged at 9,200 g for 5 min at 4°C. Thereafter, 10 μ l of the supernatant was diluted with 400 μ l of sample diluent. Each solution (100 μ l) was transferred to an antibody-coated plate and incubated at 37°C for 2 h. Subsequently, after washing five times with 400 μ l of wash solution, 100 μ l of peroxidase (POD)-conjugate solution was added to each well and incubated at room temperature for 1 h. Furthermore, after washing five times with wash solution, 100 μ l of color reagent was added to each well and incubated at room temperature in the dark for 20 min. Finally, 100 μ l of stop solution was added, and the absorbance at 450 nm was measured using a microplate reader (iMark Microplate Absorbance Reader).

2.13 | Evaluation of the effect of antitumor vaccination

All animal experiments were approved by the Ethics Committee for Animal Experiments at the School of Engineering, Nagoya University (G210593).

BALB/c mice (SLC, Japan) and BALB/c nu/nu mice (SLC, Japan) were used in this study. CT26 cells were seeded in 100-mm dishes at 3.0×10^6 cells/dish in 10 ml of RPMI 1640 medium and incubated for 24 h. The stock solution of either red-pMFC or ox-pMFC in DPBS was administered to the cell culture at a final concentration of 1.0 mg/ml. After 24 h of incubation, the cells were collected using trypsin. In total, 3.0×10^6 CT26 cells, either untreated or treated with ox-pMFC, were inoculated subcutaneously into the left flank of mice. Thereafter, 5.0×10^5 untreated CT26 cells were inoculated into the right flank 7 days after the injection of ox-pMFC-treated CT26 cells. The incidence of tumors was monitored every 2–3 days for 30 days.

2.14 | In vivo antitumor therapy by intratumoral injection of pMFC

BALB/c mice were injected with 3.0×10^5 CT26 cells in the left flank. When the tumors reached 30–100 mm³ in size, the mice were either untreated (control) or treated with 10 mg/ml of pMFC in 100 μ l DPBS

per day on Days 0–4. Tumor sizes were monitored every 3 days, and tumor volumes were calculated as (short diameter)² × (long diameter)/2. Mice were euthanized when the tumor volume exceeded 2000 mm³.

3 | RESULTS AND DISCUSSION

3.1 | Extraction of intracellular electrons and induction of oxidative stress by pMFC

First, the penetration of pMFC into the cell membranes of murine colorectal carcinoma CT26 cells was examined. Rho-pMFC²³ was added to the CT26 cell culture, which was incubated for 1 h, followed by observation using fluorescence microscopy. The fluorescence derived from rhodamine B was observed within CT26 cells cultivated with rho-pMFC (Figure S1), indicating that pMFC penetrated the cell membrane of CT26 cells and was translocated into the cells.

Next, the ability of oxidized forms of pMFC (ox-pMFC) to receive electrons from CT26 cells was investigated. The CT26 cells were cultured in a medium containing ox-pMFC, and the time-course changes in the percentage of ox-pMFC in the medium were measured. The ox-pMFC has a maximum absorption wavelength of 625 nm, while the reduced forms of pMFC (red-pMFC) do not have absorbance at this wavelength. Therefore, the ox-pMFC percentage can be estimated by measuring the absorbance of the medium at 625 nm.^{21,23,25} The results showed that ox-pMFC decreased with time, both in the presence and absence of cells (Figure 2A). Furthermore, ox-pMFC levels decreased faster in the medium with CT26 cells than in the medium without cells. The decrease in the percentage of ox-pMFC in the medium without cells was probably due to the oxidation of the redox-active species in the medium by pMFC. These results indicated electron transfer from CT26 cells to ox-pMFC.

From a thermodynamic perspective, ox-pMFC can receive electrons from various intracellular redox species in living cells. For example, ox-pMFC can oxidize intracellular redox species, such as GSH and NAD(P)H,²⁵ leading to the induction of oxidative stress.²³ It was assumed that ox-pMFC also induces oxidative stress in CT26 cells. The intracellular ROS levels in CT26 cells were evaluated using CellROX™ Green Reagent, which can detect hydroxyl radical and superoxide anion radical.^{26,27} The intracellular ROS level increased in CT26 cells treated with ox-pMFC, whereas CT26 cells treated with red-pMFC showed the same ROS level as the control cells (Figure 2B). These results revealed electron extraction via ox-pMFC induced oxidative stress in CT26 cells.

3.2 | Effect of pMFC on the viability of CT26 cells

Ox-pMFC and red-pMFC were added to the culture medium of CT26 cells at various concentrations to evaluate the effect of the redox state of pMFC on CT26 cells. Cell viability was measured after 24 h of cultivation with pMFC (Figure 3A). No substantial decrease in viability was observed in CT26 cells cultured with red-pMFC, which

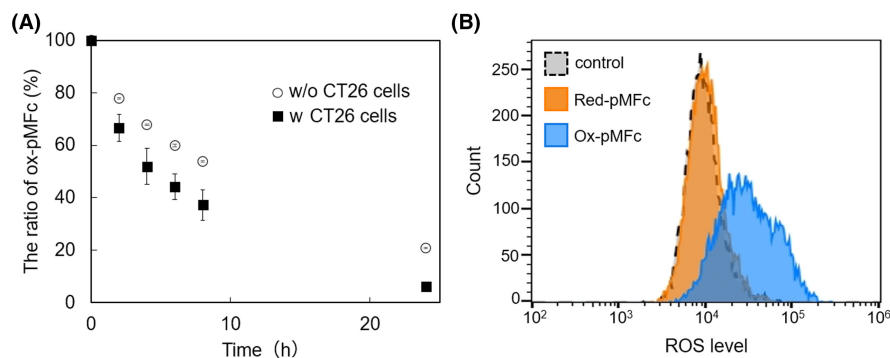


FIGURE 2 (A) Time-course changes in the percentage of ox-pMFC in the culture medium, with CT26 cells (black squares) and without CT26 cells (open circles), determined by the absorbance of culture medium at 625 nm. Ox-pMFC (1.0 mg/ml) was added to the medium both in the presence of CT26 cells (1.0×10^6 cells), and in the absence of CT26 cells. Error bars represent the average \pm SD ($n = 3$). (B) Intracellular ROS levels in CT26 cells incubated for 24 h in the culture medium with no pMFC (control) (gray dashed), with addition of 1.0 mg/ml of red-pMFC (orange), and with addition of 1.0 mg/ml of ox-pMFC (blue). CT26 cells were stained with CellROX™ Green and analyzed by flow cytometry

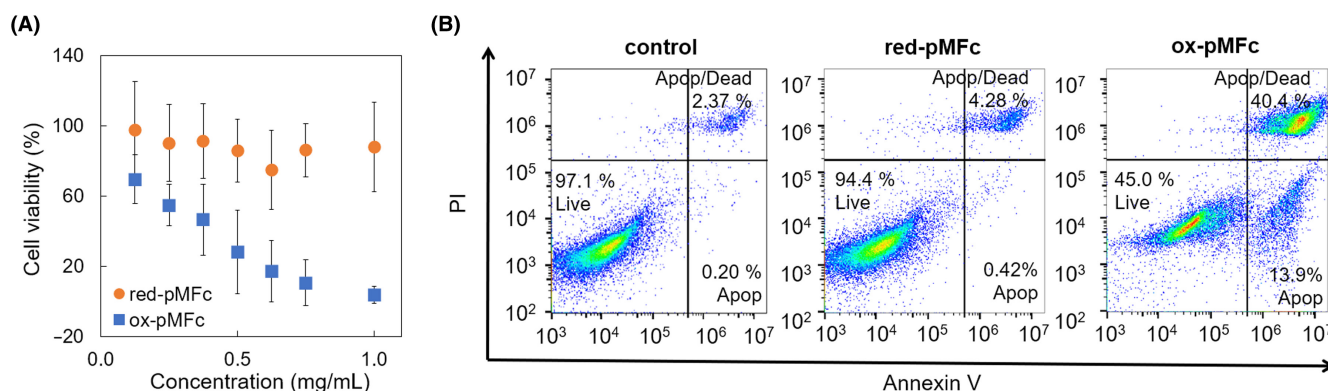


FIGURE 3 (A) Viability of CT26 cells incubated for 24 h in culture medium with the addition pMFC at various concentrations in the range 0.13–1.0 mg/ml. Cell viability was normalized by the control (culture medium with no pMFC). The data points corresponding to red-pMFC (circles) and ox-pMFC (squares) are shown. Error bars represent the average \pm SD ($n = 3$). (B) Apoptosis assay of CT26 cells incubated for 24 h in culture medium without pMFC (control), with addition of 1.0 mg/ml of red-pMFC, and 1.0 mg/ml of ox-pMFC. CT26 cells were stained with annexin V and PI and analyzed by flow cytometry

cannot receive electrons. In contrast, the viability of the cells cultured with ox-pMFC decreased in a dose-dependent manner. These results indicated that CT26 cell viability was suppressed by electron extraction by ox-pMFC. Furthermore, the induction of apoptosis in CT26 cells was investigated. An apoptosis assay was performed on CT26 cells cultured with pMFC by co-staining with annexin V and PI. Whereas most of the cells cultured without pMFC or with red-pMFC were viable, only those cultured with ox-pMFC showed an increase in the percentage of early and late apoptotic cells (Figure 3B). These results indicated that ox-pMFC induced apoptosis in CT26 cells.

3.3 | Analysis of DAMPs

Considering that oxidative stress is involved in ICD induction, it was hypothesized that ox-pMFC could induce ICD in CT26 cells. When cancer cells undergo ICD, they present or release a group of molecules called DAMPs such as CRT, ATP, and HMGB1. DAMPs attract

immature dendritic cells and promote their maturation, followed by the activation of T cell-mediated antitumor immune reactions. In this study, the expression levels of CRT on the surface of the CT26 cell membrane and the concentrations of released ATP and HMGB1 in the cell culture medium were measured. Based on flow cytometry with the CRT antibody, the expression level of CRT increased only when the cells were cultivated with ox-pMFC (Figure 4A). Moreover, the released levels of ATP (Figure 4B) and HMGB1 (Figure 4C) increased in the cell culture medium cultivated with ox-pMFC. These results indicated that ox-pMFC induced ICD-associated release of DAMPs in CT26 cells.

3.4 | In vivo vaccine-like effect of pMFC-treated CT26 cells

Although CRT exposure on the cell surface and the release of ATP and HMGB1 in the culture medium are reliable hallmarks of ICD, in

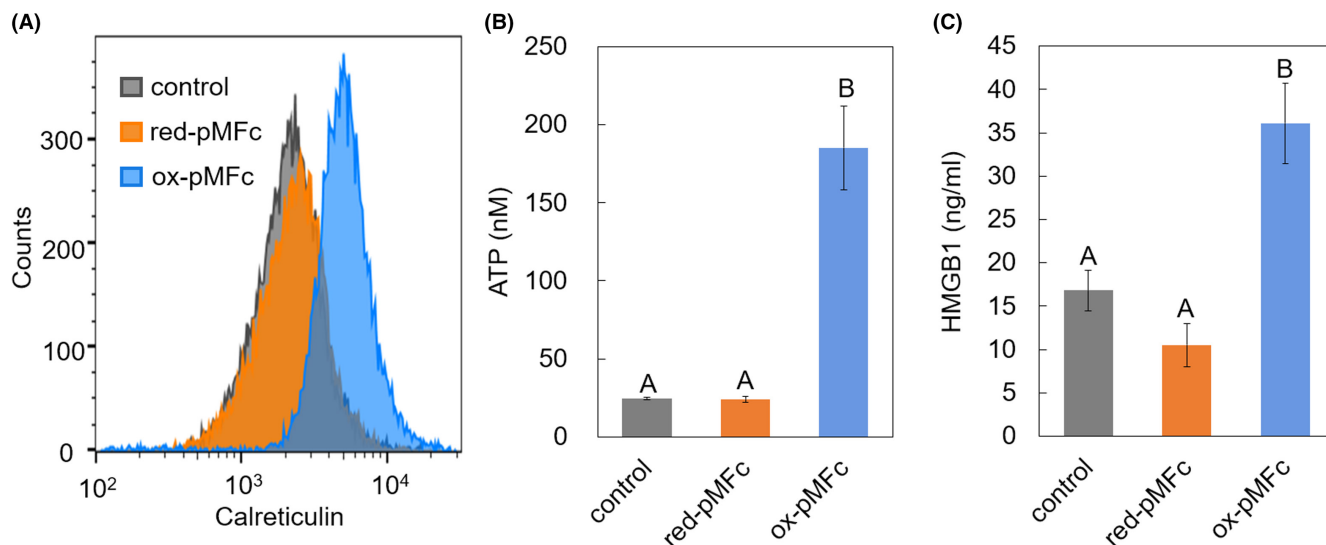


FIGURE 4 (A) Expression levels of CRT in CT26 cells cultured for 24 h in culture medium with no pMFC (control), with 1.0 mg/ml red-pMFC, or with 1.0 mg/ml ox-pMFC. (B) ATP concentration in the supernatant of culture medium in which CT26 cells were cultured with no pMFC (control), with 1.0 mg/ml red-pMFC, or with 1.0 mg/ml ox-pMFC for 24 h. Error bars represent the average \pm SD ($n = 3$). (C) HMGB1 concentration in the supernatant of culture medium in which CT26 cells were cultured, with no pMFC (control), with 1.0 mg/ml red-pMFC, or with 1.0 mg/ml ox-pMFC, for 24 h. Error bars represent the average \pm SD ($n = 3$). Welch *t*-test with Bonferroni correction was used to compare the three conditions. Different letters (A, B) represent significant difference ($p < 0.05$)

vivo vaccination experiments are needed to confirm that ox-pMFC is a genuine ICD inducer.³ CT26 cells cultured with ox-pMFC for 24 h were injected subcutaneously into the left flank of immunocompetent BALB/c mice and immunodeficient BALB/c nu/nu mice. The injected CT26 cells did not form tumors probably because ox-pMFC-treated cells underwent apoptosis 24 h after the *in vitro* treatment (Figure 3B). One week later, nontreated CT26 cells were injected into the right flank of the mice, and subsequent tumor formation was monitored for 30 days. Control groups of immunocompetent BALB/c mice and immunodeficient BALB/c nu/nu mice, not injected with ox-pMFC-treated cells, were also injected with nontreated CT26 cells; the subsequent tumor formation was monitored for 30 days. In the control group of BALB/c mice, tumors were observed in mice ($n = 6$) on Day 7, and all six mice had tumors by Day 11 (Figure 5). In contrast, in the BALB/c mice group previously injected with ox-pMFC-treated CT26 cells, no tumor formation was observed by the subsequently injected nontreated CT26 cells in any of the mice until Day 26. Furthermore, the immunodeficient BALB/c-nu/nu mice, injected with ox-pMFC-treated CT26 cells, showed a similar profile of rechallenged tumorigenesis as the control groups of both BALB/c and BALB/c-nu/nu mice. These results indicated that ox-pMFC induced ICD in CT26 cells, therefore activating antitumor immunity and inhibiting tumorigenesis in BALB/c mice.

To date, few reports have shown that ferrocene and its derivatives induce ICD.^{28,29} Recently, Wang et al.²⁹ reported ferroptosis-induced cancer immunity caused by a ferrocene-appended iridium (III) diphosphine complex, Ir1. Ferroptosis is a novel type of nonapoptotic cell death caused by an increased level of ROS and resulting lipid peroxidation.³⁰ They showed that Ir1 localized in lysosomes, which offer an acidic environment, and caused a Fenton-like reaction by

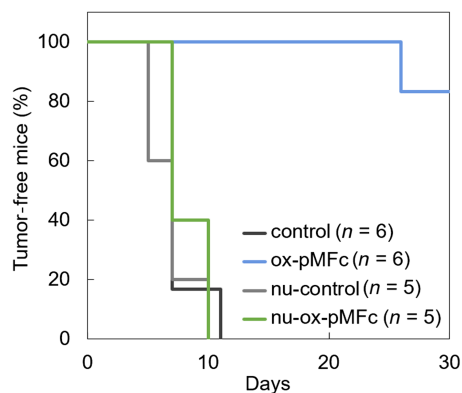


FIGURE 5 Time course of the percentages of tumor-free mice, after injection of nontreated CT26 cells, in the groups of mice of the following category: BALB/c mice (control), BALB/c mice injected with ox-pMFC-treated CT26 cells (ox-pMFC), BALB/c nu/nu mice (nu-control), BALB/c nu/nu mice injected with ox-pMFC-treated CT26 cells (nu-ox-pMFC). The ox-pMFC-treated CT26 cells were injected into the left flank of mice (except the control and nu-control groups). At 7 days after the injection, nontreated CT26 cells were injected into the right flank of the mice, and the incidence of tumors was monitored every 2–3 days. Each group included five or six mice

ferrocene, leading to ROS production and cell death. In contrast, amphiphilic MPC polymers can shuttle between the intracellular and extracellular milieu across the cell membrane via a simple diffusion process,^{18,20} suggesting that pMFC was not localized in lysosomes. Moreover, red-pMFC did not affect the ROS level (Figure 2B) and cell viability (Figure 3A). Therefore, we deemed the contribution of the Fenton-like reaction to be trivial for pMFC. Our results showed

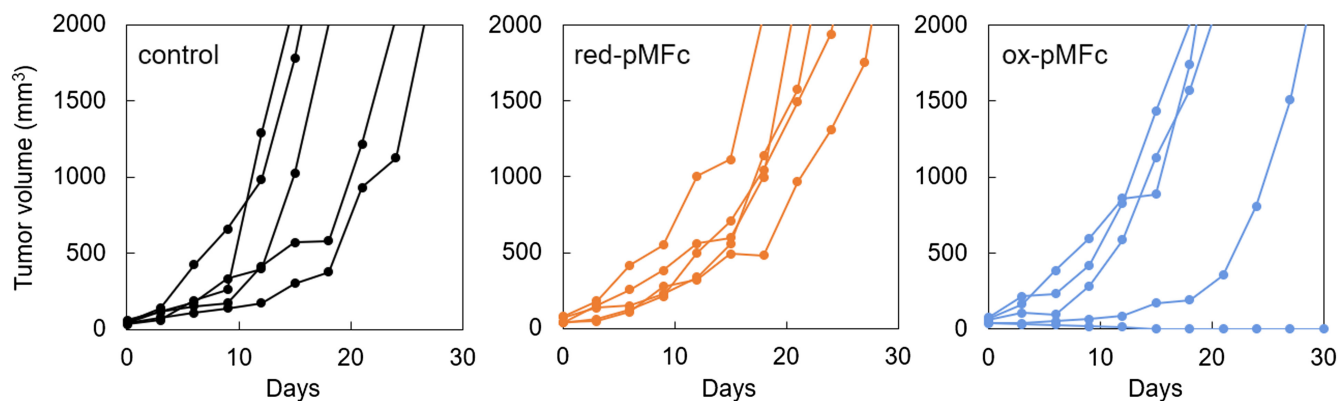


FIGURE 6 Time course of tumor volume in mice with subcutaneous CT26 tumors. When the tumors reached 30–100 mm³ in size, mice were either untreated (control), treated with red-pMFc, or treated with ox-pMFc. Tumor sizes were monitored every 3 days using a caliper and tumor volumes were calculated as (short diameter)² × (long diameter)/2. Each group included five mice

that ox-pMFc induced apoptotic cell death via oxidative stress and the resultant ICD. We surmise that the mechanism of ICD induced by ox-pMFc is different from that of Ir1 and further investigation is required to elucidate the mechanism. From a mechanistic viewpoint, it is also important to elucidate the differences in the cell membrane permeability between red-pMFc and ox-pMFc. However, it is difficult to quantify cellular uptake using fluorescence labeling because ferrocene units can quench fluorescent molecules.³¹ Methods for quantitative evaluation of cellular uptake of pMFc remain to be developed.

3.5 | In vivo therapeutic effect of pMFc

The effect of pMFc on established tumors was evaluated. CT26 cells were injected subcutaneously into BALB/c mice to prepare model mice with tumors. Tumor size was measured every 3 days and, when the tumor size reached 30–100 mm³, either red-pMFc or ox-pMFc was directly injected into tumors. A control group of mice with tumors was untreated; their tumor size was also measured every 3 days. In the group of mice injected with ox-pMFc, the tumor sizes were suppressed to <500 mm³ in two out of five mice at Day 21, and one of them showed complete regression (Figures 6 and S2A). In the untreated control group and the group of mice injected with red-pMFc, all mice had tumors >500 mm³ on Day 21. To further analyze the antitumor effect of ox-pMFc, we calculated the tumor growth rate during pMFc administration (Figure S3). The group treated with ox-pMFc showed a lower tumor growth rate, although not statistically significant. These results suggest that ox-pMFc can directly inhibit tumor growth. No obvious changes were observed in the body weights of either the ox-pMFc- or red-pMFc-injected groups (Figure S2B). These results imply that ox-pMFc is effective for in vivo tumor treatment. In the present study, the antitumor effects of ox-pMFc administration were somewhat limited, and the therapeutic protocol (including dosage, concentration and frequency of administration) should be optimized before clinical trials. The limitation of antitumor effects can be attributed to the uneven distribution of

pMFc in tumors. Improving diffusivity and retention of pMFc within tumors by modifying the polymer structure would improve the in vivo antitumor effect. Moreover, modulation of the redox properties of the redox-active monomer may also improve the anticancer potency. Because the redox phospholipid polymers studied here were random copolymers that can be synthesized by conventional free radical polymerization, redox phospholipid polymers equipped with functional units can readily be developed by the judicious selection of appropriate monomers. Therefore, the therapeutic efficiency is expected to be improved by a more sophisticated polymer design, such as introducing tumor retention units and optimizing redox-active units. Considering recent advances in cancer immunotherapy, combining immune checkpoint inhibitors, such as anti-CTLA4 and anti-PD-1 antibodies,³² would be another promising strategy to augment the therapeutic outcome of redox phospholipid polymers.

4 | CONCLUSION

A rational design strategy for ICD inducers is highly sought after. In this study, we showed that the ferrocene-containing redox phospholipid polymer (ox-pMFc) induced ICD, evidenced by the release of DAMPs and the vaccine-like effect of pMFc-treated murine colorectal carcinoma CT26 cells. Moreover, the in vivo cancer therapy in a mouse tumor model implied that ox-pMFc is effective in treating tumors. These results suggest that cell-penetrating phospholipid polymers containing ferrocene units are promising ICD inducers. This study will serve as a guideline for designing new ICD-inducing polymers and contribute to the development of novel cancer therapies.

ACKNOWLEDGMENTS

This research was supported by JSPS KAKENHI Grant No. 20K22465 (M.K.), The Public Interest of Tatematsu (M.K.), and The Nitto Foundation (M.K.)

DISCLOSURE

The authors have no conflict of interest.

ETHICAL APPROVAL

Approval of the research protocol by an Institutional Reviewer Board: N/A.

Informed Consent: N/A.

Registry and the Registration No: N/A.

Animal Studies: Ethics Committee for Animal Experiments at the School of Engineering, Nagoya University (G210593).

ORCID

Masahiro Kaneko  <https://orcid.org/0000-0002-8309-4086>

Akira Ito  <https://orcid.org/0000-0001-8393-0518>

REFERENCES

- Krysko DV, Garg AD, Kaczmarek A, Krysko O, Agostinis P, Vandenabeele P. Immunogenic cell death and DAMPs in cancer therapy. *Nat Rev Cancer*. 2012;12:860-875.
- Galluzzi L, Buqué A, Kepp O, Zitvogel L, Kroemer G. Immunogenic cell death in cancer and infectious disease. *Nat Rev Immunol*. 2017;17:97-111.
- Fucikova J, Kepp O, Kasikova L, et al. Detection of immunogenic cell death and its relevance for cancer therapy. *Cell Death Dis*. 2020;11:1.
- Gardai SJ, McPhillips KA, Frasch SC, et al. Cell-surface calreticulin initiates clearance of viable or apoptotic cells through trans-activation of LRP on the phagocyte. *Cell*. 2005;123:321-334.
- Obeid M, Tesniere A, Ghiringhelli F, et al. Calreticulin exposure dictates the immunogenicity of cancer cell death. *Nat Med*. 2007;13:54-61.
- Elliott MR, Chekeni FB, Trampont PC, et al. Nucleotides released by apoptotic cells act as a find-me signal to promote phagocytic clearance. *Nature*. 2009;461:282-286.
- Medina CB, Ravichandran KS. Do not let death do us part: 'find-me' signals in communication between dying cells and the phagocytes. *Cell Death Differ*. 2016;23:979-989.
- Apetoh L, Ghiringhelli F, Tesniere A, et al. Toll-like receptor 4-dependent contribution of the immune system to anticancer chemotherapy and radiotherapy. *Nat Med*. 2007;13:1050-1059.
- Yang D, Chen Q, Yang H, Tracey KJ, Bustin M, Oppenheim JJ. High mobility group box-1 protein induces the migration and activation of human dendritic cells and acts as an alarmin. *J Leukoc Biol*. 2007;81:59-66.
- Van Loenhout J, Peeters M, Bogaerts A, Smits E, Deben C. Oxidative stress-inducing anticancer therapies: taking a closer look at their immunomodulating effects. *Antioxidants*. 2020;9:1.
- Li C, Zhang Y, Yan S, et al. Alternol triggers immunogenic cell death via reactive oxygen species generation. *Onco Targets Ther*. 2021;10:10. doi:10.1080/2162402X.2021.1952539
- Tesniere A, Schlemmer F, Boige V, et al. Immunogenic death of colon cancer cells treated with oxaliplatin. *Oncogene*. 2010;29:482-491.
- Casares N, Pequignot MO, Tesniere A, et al. Caspase-dependent immunogenicity of doxorubicin-induced tumor cell death. *J Exp Med*. 2005;202:1691-1701.
- Terenzi A, Pirker C, Keppler BK, Berger W. Anticancer metal drugs and immunogenic cell death. *J Inorg Biochem*. 2016;165:71-79.
- Ishihara K, Ueda T, Nakabayashi N. Preparation of phospholipid polymers and their properties as polymer hydrogel membranes. *Polym J*. 1990;22:355-360.
- Ishihara K. Revolutionary advances in 2-methacryloyloxyethyl phosphorylcholine polymers as biomaterials. *J Biomed Mater Res Part A*. 2019;107:933-943.
- Sikkema J, de Bont JA, Poolman B. Mechanisms of membrane toxicity of hydrocarbons. *Microbiol Rev*. 1995;59:201-222.
- Goda T, Goto Y, Ishihara K. Cell-penetrating macromolecules: direct penetration of amphipathic phospholipid polymers across plasma membrane of living cells. *Biomaterials*. 2010;31:2380-2387.
- Goda T, Imaizumi Y, Hatano H, Matsumoto A, Ishihara K, Miyahara Y. Translocation mechanisms of cell-penetrating polymers identified by induced proton dynamics. *Langmuir*. 2019;35:8167-8173.
- Goda T, Miyahara Y, Ishihara K. Phospholipid-mimicking cell-penetrating polymers: principles and applications. *J Mater Chem B*. 2020;8:7633-7641.
- Nishio K, Nakamura R, Lin X, et al. Extracellular electron transfer across bacterial cell membranes via a cytochrome redox-active polymer. *ChemPhysChem*. 2013;14:2159-2163.
- Wu JS, Toda K, Tanaka A, Sanemasa I. Association constants of ferrocene with cyclodextrins in aqueous medium determined by solubility measurements of ferrocene. *Bull Chem Soc Jpn*. 1998;71:1615-1618.
- Kaneko M, Ishikawa M, Ishihara K, Nakanishi S. Cell-membrane permeable redox phospholipid polymers induce apoptosis in MDA-MB-231 human breast cancer cells. *Biomacromolecules*. 2019;20:4447-4456.
- Kaneko M, Ishikawa M, Nakanishi S, Ishihara K. Anticancer activity of cell-penetrating redox phospholipid polymers. *ACS Macro Lett*. 2021;10:926-932.
- Ishikawa M, Kawai K, Kaneko M, Tanaka K, Nakanishi S, Hori K. Extracellular electron transfer mediated by a cytochrome redox polymer to study the crosstalk among the mammalian circadian clock, cellular metabolism, and cellular redox state. *RSC Adv*. 2020;10:1648-1657.
- Choi H, Yang Z, Weisshaar JC. Single-cell, real-time detection of oxidative stress induced in *Escherichia coli* by the antimicrobial peptide CM15. *Proc Natl Acad Sci USA*. 2015;112:E303.
- McBee ME, Chionh YH, Sharaf ML, Ho P, Cai MWL, Dedon PC. Production of superoxide in bacteria is stress- and cell state-dependent: a gating-optimized flow cytometry method that minimizes ROS measurement artifacts with fluorescent dyes. *Front Microbiol*. 2017;8:459.
- Zhang J, Yang J, Zuo T, et al. Heparanase-driven sequential released nanoparticles for ferroptosis and tumor microenvironment modulations synergism in breast cancer therapy. *Biomaterials*. 2021;266:120429.
- Wang WJ, Ling YY, Zhong YM, Li ZY, Tan CP, Mao ZW. Ferroptosis-enhanced cancer immunity by a ferrocene-appended iridium(III) Diphosphine complex. *Angew Chem Int Ed*. 2022;61:e202115247.
- Kuang F, Liu J, Tang D, Kang R. Oxidative damage and antioxidant defense in ferroptosis. *Front Cell Dev Biol*. 2020;8:969.
- Fery-Forgues S, Delavaux-Nicot B. Ferrocene and ferrocenyl derivatives in luminescent systems. *J Photochem Photobiol A Chem*. 2000;132:137-159.
- Seidel JA, Otsuka A, Kabashima K. Anti-PD-1 and anti-CTLA-4 therapies in cancer: mechanisms of action, efficacy, and limitations. *Front Oncol*. 2018;8:86.

SUPPORTING INFORMATION

Additional supporting information can be found online in the Supporting Information section at the end of this article.

How to cite this article: Kaneko M, Yamaguchi A, Ito A. Induction of immunogenic cell death in murine colon cancer cells by ferrocene-containing redox phospholipid polymers. *Cancer Sci*. 2022;113:3558-3565. doi: [10.1111/cas.15525](https://doi.org/10.1111/cas.15525)